

Photometric analysis of a 100 m ice core from Asuka Camp, East Antarctica : Preliminary results

Nobuhiko AZUMA¹, Kumiko GOTO-AZUMA² and Masayosi NAKAWO³

¹ Department of Mechanical Engineering, Nagaoka University of Technology, Nagaoka, Niigata 940–21 Japan

² Nagaoka Institute of Snow and Ice Studies, Suyosi, Nagaoka, Niigata 940 Japan

³ Institute for Hydrospheric-Atmospheric Sciences, Nagoya University, Nagoya 464–01 Japan

(Received April 15, 1994 ; Revised manuscript received July 23, 1994)

Abstract

The reflective light intensity was measured continuously on a vertically split flat surface of a 100 m ice core from Asuka Camp, East Antarctica with a newly developed photometric device for rapid stratigraphic analyses. The data obtained by the photometric measurement were compared with the density data and visual stratigraphy. The reflectivity and its standard deviation showed good correlations with density and grain size respectively at shallower part of the core. This fact suggests that a new photometric method provides us stratigraphic information such as the degree of depth hoar development.

1. Introduction

In order to measure the continuous records of physical properties of ice core such as density, porosity and grain size, we are developing a photometric method. Here we present preliminary results of the photometric measurement made on a 100 m core from Asuka camp, East Antarctica. Asuka Camp is located at lat.71°31'S, long.24°8'E, and 930 m a.s.l.(Fig. 1). Mean annual temperature is –20°C. Accumulation rate measured by snow stake method is about 0.19 m a⁻¹ of ice. A 103 m length and 10 cm diameter ice core was recovered during April 1989. The photometric measurement was carried out in a cold room during 1992/1993.

2. Methods

2.1. Core sampling

The core was split vertically by a bandsaw and a half was used for photometric analysis, density measurement, ECM (Electrical Conductivity Measurements) and oxygen isotope measurement. The other half was provided for chemical analyses. A half core for photometric measurement and ECM was mi-

crotoned on a split surface to provide a flat and clean surface for the measurements. After these measurements, the core was cut into lengths of 4 cm long along core axis for density measurement. These samples were afterward melted and provided for oxygen isotope measurement. Density was determined by measuring the size and weight of each sample. All these procedures were carried out in a cold room at a temperature of –15°C. Detailed analyses of this core including chemical data will be discussed elsewhere.

2.2. Photometric method

Figure 2 shows a schematic diagram of the measuring system used. A photo sensor connected to a light source (a halogen lamp) by an optical fiber was moved over a flat surface of a core along the core axis. A light beam emitted from the optical fiber was irradiated on the surface of the core at an angle of 45 degree. The irradiated area is approximated by an ellipse with axes of 7 mm by 5 mm with the minor axis oriented along the scanning direction. The reflective light intensity from irradiated area was detected by a photo-diode (Fig. 2) and recorded by an x-y recorder through a photo-sensor amplifier. The x-position of the irradiated area was measured by a rotary encoder

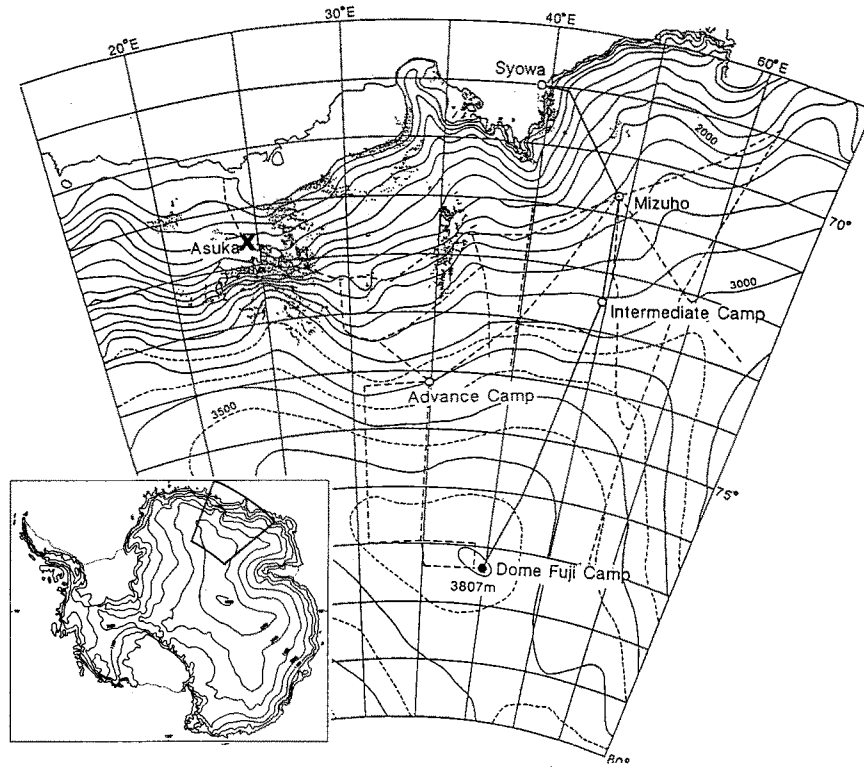


Fig. 1. Location of Asuka Camp (x).

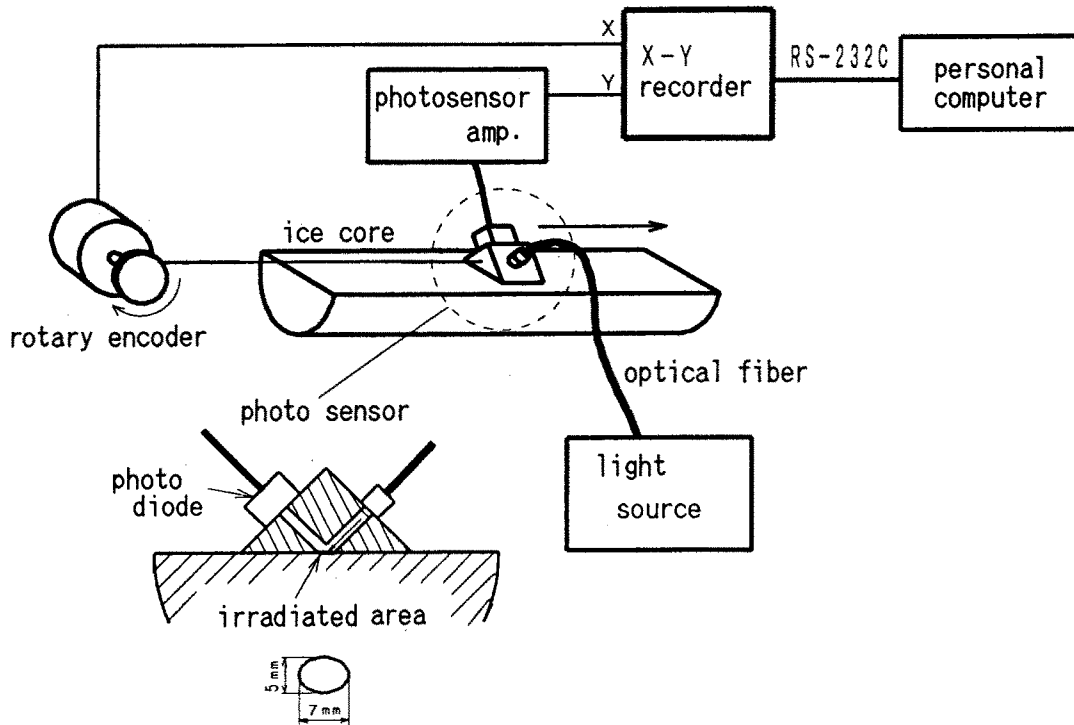


Fig. 2. A schematic diagram of the photometric measurement system.

and inputted into the x-y recorder.

After each run the data were stored on a micro floppy disc in a personal computer. Due to the slow response time (0.1 sec) of the photo-sensor amplifier, short-time variations of the reflected intensity was attenuated. With a sliding velocity of 1 cm s^{-1} , the depth resolution was around 1 mm. Before each run the sliding plane of the photo sensor was contacted a mirror and the reflective intensity was measured in order to obtain the incident light intensity on the core surface and to maintain its value a constant for every run.

3. Results

Figure 3 shows the overall depth profiles of the density (3-a) and the reflectivity (3-b) which was obtained by dividing the reflective light intensity R by the incident light intensity I_0 . Heavier lines (zig-zag lines) indicate 50 cm means of each data. Thinner lines show the regression lines. Pore close-off occurred at about 40–50 m. The reflectivity gradually decreased with depth until about 50 m and increased again below 50 m with a large fluctuation. The

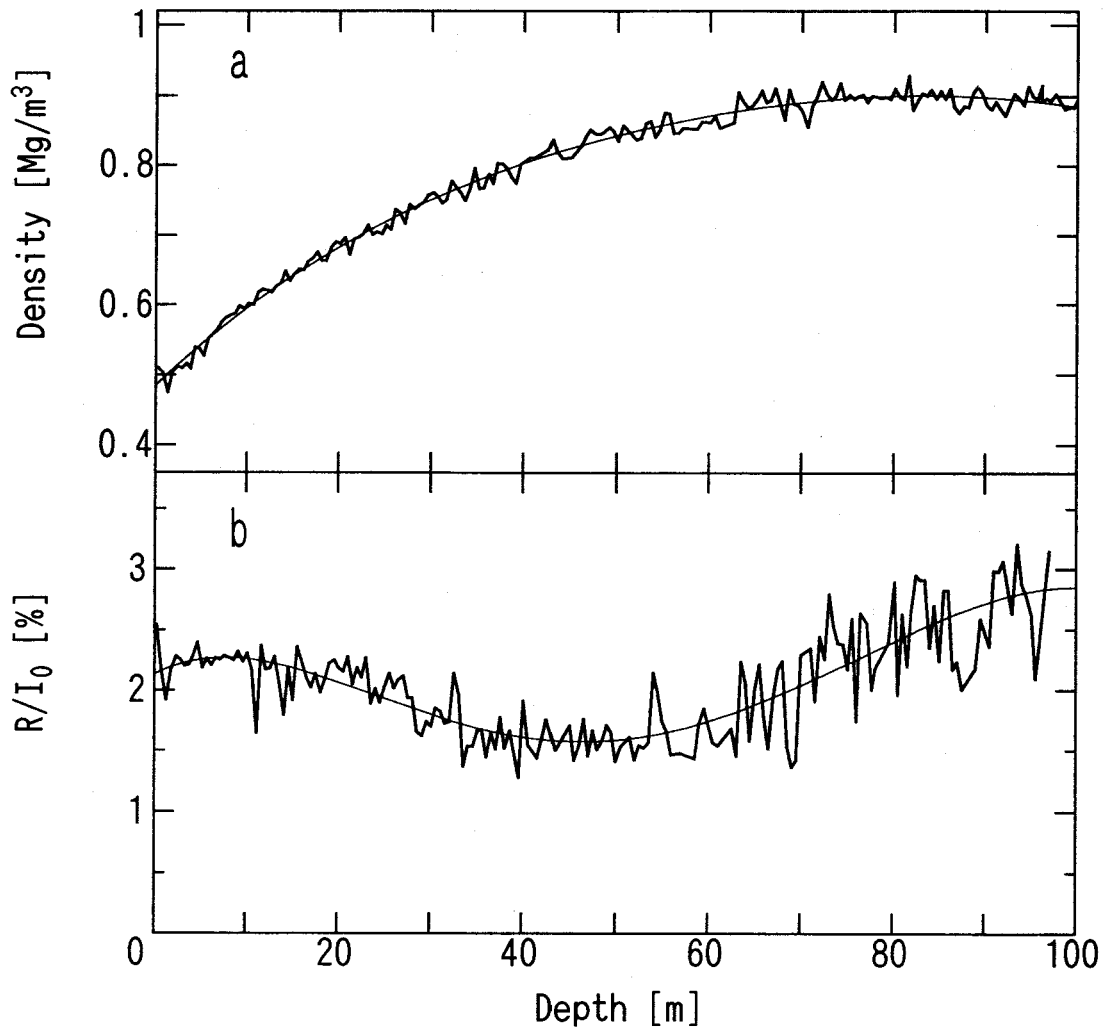


Fig. 3. Depth profiles of the density (a) and the reflectivity (b). Heavy lines show a 50 cm mean of each data. Thin lines show regression lines of the fifth order.

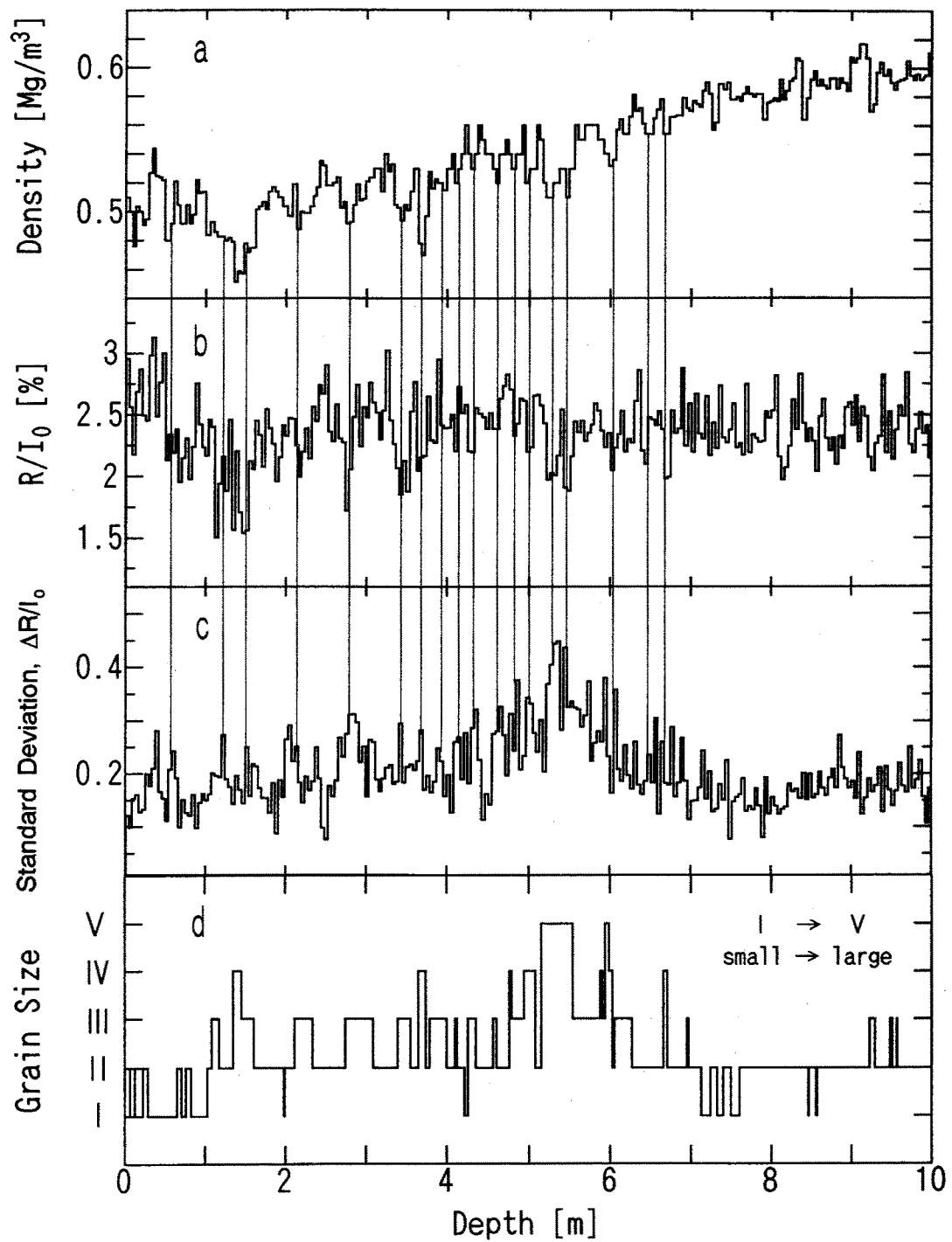


Fig. 4. Comparison of the stratigraphic features in the photometric measurement signals for a top 10 m core ; (a) density, (b) reflectivity, (c) standard deviation of the reflectivity and (d) grain size. I : 0–0.5 mm, II : 0.5–1.0 mm, III : 1.0–1.5 mm, IV : 1.5–2.0 mm, V : 2.0 mm~. Vertical thin lines indicate a good correlation among them.

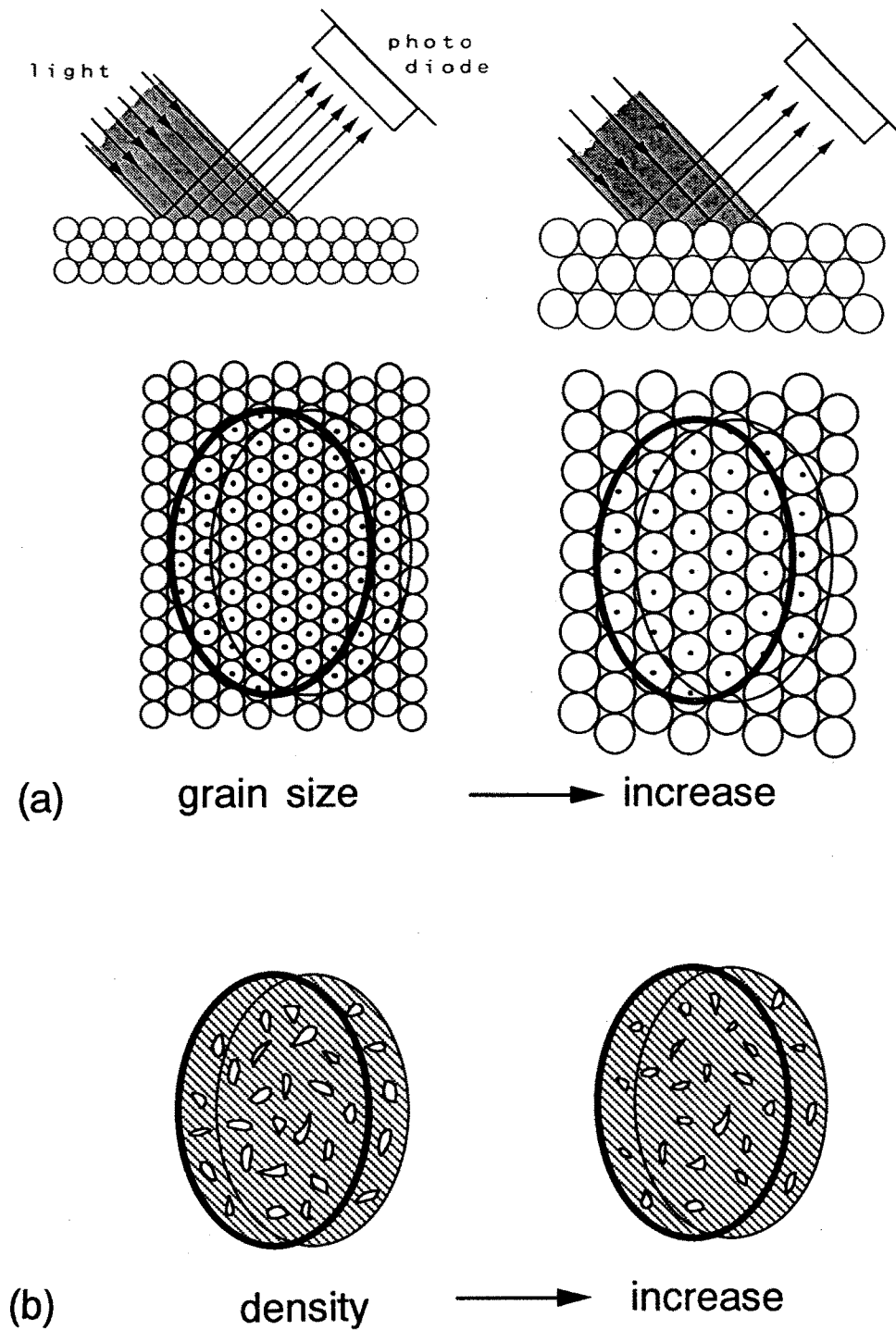


Fig. 5. Dependence of reflective area within an irradiated area (inside of an ellipse) on the grain size. Black spots and hatched area indicate the effective reflection area. (a) Shallower depth ; 0 - 7 m, and (b) deep depth ; 50 m-100 m.

depth-density plot shows large negative deviations of 50 cm mean data from the regression lines at the depths around 60 m, 70 m and 90 m. At these depths the reflectivity also deviated largely in a negative manner.

The detailed depth profiles of density, reflectivity, standard deviation of reflectivity and grain size for the top 10 m of the core are shown in Fig. 4-a, 4-b, 4-c and 4-d respectively. Each data point shows the mean value of 4 cm interval.

Grain size measurement was made on the bulk core using a grain size gauge. Therefore its depth profile was indicated by the relative grade.

There is a clear positive correlation between density and reflectivity until about 7 m, and below this depth the correlation become unclear. Figure 4 also indicates a good correlation between the standard deviation of reflectivity and grain size. Large standard deviation corresponds to large grain size. These depths also corresponded to less reflectivity and less density. Visual observation of the core revealed that these depths were characterized by clear development of depth hoar.

4. Discussion and Conclusions

Main part of reflective light is attributed to the reflection from surface layer grains. Within the surface of each grain, only the reflective light from the area which oriented suitably to the incident direction reaches a photo-diode.

Figure 5 shows schematically the reflective area within the irradiated area. To simplify the discussion, a grain is assumed to be spherical. A black spot in each grain indicates the effective reflection area. As grain size increases, the sum of the effective reflection area decreases because the total number of irradiated grains decreases. Hence reflectivity is reversely correlated with grain size. When the irradiated area slides 1 mm as shown by the ellipses with thin lines, the variation of the total effective reflection area is larger for larger grains in size. This leads to the greater standard deviation of reflectivity for larger grains.

At shallower part of the core (*i.e.* upper 7 m) where the densification had not proceeded yet so that the effective reflection area of each grain can be regarded as a point, the lower reflectivity and higher standard deviation corresponded to larger grain size, and vice versa.

At the depth between about 7 m and 50 m, the increase of grain size with depth causes the reflectivity to decrease with depth in above mentioned manner. On the other hand, the increase of the effective reflection area due to the densification with depth causes the reflectivity to increase with depth. As a result, a clear correlation disappears with depth.

At the depth below 50 m where air bubbles have been already isolated, the increase of flat surface except for concave of air bubbles causes the increase of reflectivity as the densification proceeds with depth as can be seen in Fig. 5b. This suggests that the distinctive low values of reflectivity around 60 m, 70 m and 90 m could be caused by high porosity at those depths. This idea was supported by the visual observation and the density measurement.

Alley *et al.* (1982) reported that the coarse firn layer characterized by large grains and low density was preserved down to several tens meter depth although the difference in density between coarse and fine firn at a given depth decreases rapidly with depth. It was also reported that these coarse firn layers had been originated in the top 0.2 m by the depth hoar development (Alley and Bentley, 1988). Therefore, the low density layers with low reflectivity around 60 m, 70 m and 90 m in Asuka core seem to be caused by the anomalous climate condition there at the time when those layers were near the surface.

During our one year stay at Asuka Camp, we had three severe storms with significant snow deposit. All snow deposit concentrated in summer and autumn (*i.e.* January to April) and this is a typical pattern of snow deposition around Asuka Camp according to the available meteorological data records. In winter snow seldom deposits and the strong wind packs surface snow densely.

In this region, an ice crust develops very well during late-winter to early-summer (Fujii, 1979; Fujii and Kusunoki, 1982). Fujii (1979) investigated the mechanism of the ice crust development in detail and concluded that the increase of diagenetic mass transportation due to increase of the solar radiation in spring caused the developments of an ice crust and depth hoar just below the crust.

We carried out pit studies at same place in Asuka Camp at August 1989 and February 1990. The crust surface of February was the same one of August because of no snow deposition between them. From the pit observations it was found that the depth hoar below the crust in February was developed strongly

whereas the depth hoar layer could not be recognized clearly below the crust surface in August. This result supports Fujii's conclusions.

Consequently, in this region where the snow accumulation is characterized by summer/autumn deposition pattern, coarse firn layer with larger grain and lower density may be regarded as an annual boundary. Vertical thin lines in Fig. 4, therefore, seem to indicate the annual boundaries, which were determined from well correlated position among density, reflectivity and its standard deviation.

This analysis gives us an accumulation rate of 0.22 m a^{-1} of ice. From depth-density profile we obtained an accumulation rate of 0.24 m a^{-1} of ice using the Herron-Langway's equation (Herron and Langway, 1980). Snow stake observation for recent three years gives a value for accumulation rate of 0.19 m a^{-1} of ice. These values are in good agreement with estimated value from the photometric analyses. Although the further interpretation of the photometric data in terms of grain size, grain shape, internal surface area and density is necessary, this photometric method has a potential to investigate the stratigraphy of ice cores rapidly and quantitatively.

Acknowledgments

The authors thank T. Matuda, H. Hara and H. Yamaguchi for their considerable work in photometric measurements. Also we thank Y. Fujii for helpful comments.

References

1. Alley, R. B., Bolzan, J. F. and Whillans, I. M. (1982) : Polar firn densification and grain growth. *Ann. Glaciol.*, **3**, 7–11.
2. Alley, R. B. and Bentley, C. R. (1988) : Ice-core analysis on the Siple coast of West Antarctica. *Ann. Glaciol.*, **11**, 1–7.
3. Fujii, Y. (1979) : Sublimation and condensation at the ice sheet surface of Mizuho Station, Antarctica. *Antarc. Rec.*, **67**, 51–63.
4. Fujii, Y. and Kusunoki, K. (1982) : The role of sublimation and condensation in the formation of ice sheet surface at Mizuho Station, Antarctica. *J. Geophys. Res.*, **87**, 4293–4300.
5. Herron, M. M. and Langway, C. C. Jr. (1980) : Firn densification : An empirical model. *J. Glaciol.*, **25**, 373–385.